Reflectionless tunneling in ballistic normal-metal−superconductor junctions

M. Schechter, Y. Imry, and Y. Levinson

Department of Condensed Matter Physics, The Weizmann Institute of Science, Rehovot 76100, Israel

(Received 18 April 2001; revised manuscript received 20 August 2001; published 21 November 2001)

We investigate the phenomenon of reflectionless tunneling in ballistic normal-metal−superconductor (NS) structures using a semiclassical formalism. It is shown that applied magnetic field and superconducting phase difference both impair the constructive interference leading to this effect, but in a qualitatively different way. This is manifested both in the conductance and in the shot noise properties of the system considered. Unlike diffusive systems, the features of the conductance are sharp and enable fine spatial control of the current, as well as single-channel manipulations. We discuss the possibility of conducting experiments in ballistic semiconductor-superconductor structures with smooth interfaces and some of the phenomena, specific to such structures, that could be measured. A general criterion for the barrier at NS interfaces, though large, to be effectively transparent to pair current is obtained.

I. INTRODUCTION

One of the most interesting phenomena in hybrid diffusive normal-metal−superconductor structures is reflectionless tunneling. This phenomenon manifests itself as a zero-bias peak in the differential conductance of a diffusive normal metal slab connected to a superconductor via a tunnel barrier with low transmission probability Γ.[1,2] van Wees *et al.*[3] used a path integral picture to suggest and explain the effect of reflectionless tunneling. They show that the enhanced conductance at zero bias is due to electron-hole coherence in trajectories that, due to the disorder in the normal metal, hit the barrier at the normal-metal−superconductor (NS) interface many times. This results in the barrier being effectively transparent to pair current.

In this paper we show that the phenomenon of reflectionless tunneling exists also in ballistic systems, the requirement being the existence of multiple reflections from the NS interface due to the geometry of the structure. As in diffusive systems, we find an enhanced NS conductance for zero bias and zero magnetic field. We show that the magnetic field (H), finite energy and voltage, and superconducting phase difference (Φ_s) impair the constructive interference leading to the enhanced NS conductance, but applying the superconducting phase difference has qualitatively different consequences than applying a finite magnetic field or voltage.

We show that the ballistic nature of the system gives rise to pronounced and delicate features, which are not averaged over as in the case of diffusive systems. This results in new measurable phenomena, such as sharp *peaks* in the NS conductance as new channels open and quasiperiodicity of the conductance as a function of magnetic field. We also demonstrate the possibility, specific to ballistic systems, to conduct detailed manipulations such as extracting out a single channel from a normal metal (semiconductor) waveguide or extracting the current at a given position along the waveguide.

The ballistic regime in semiconductor-superconductor hybrid structures was investigated recently experimentally.[4−10] Unlike the case in normal-metal−superconductor structures, where sharp boundaries are made that enable specular reflection at the NS interface,[11,12] in semiconductor-superconductor interfaces specular reflection is sacrificed for the purpose of lowering the barrier at the interface, thus increasing the Andreev reflection probability. We here raise the possibility to conduct experiments in ballistic semiconductor-superconductor structures with a sharp interface and a long elastic mean free path. Though indeed the transmission probability of the barrier would then be small, the electron-hole coherence over long trajectories results in a large Andreev reflection probability, as we show below. Thus, one can have strong proximity while preserving the ballistic nature of the system. Other systems which seem favorable for the realization of ballistic NS structures with specular reflection at the interface are the recently investigated organic molecular crystals.[13,14] In these systems the NS transition could be realized by applying a space-dependent gate voltage.

The paper is arranged as follows: In Sec. II we introduce the formalism and the structure we consider, obtain the expressions for the three-terminal conductances in terms of $R_{he}(N)$, the Andreev reflection probability of a trajectory that hits the interface N times, and calculate this probability for zero magnetic field. In Sec. III we show that for a short slab the NS conductance has sharp *peaks* as channels open. In Secs. IV and V we calculate $R_{he}(N)$ and the linear conductances as a function of H (IV) and Φ_s in a similar SNS structure (V). In Sec. VI we calculate the shot noise in both structures, as a function of H and Φ_s. In Sec. VII we consider diffusive systems and demonstrate the connection between the effect of reflectionless tunneling in diffusive and ballistic systems. Throughout the paper we consider zero temperature and use the model in which the superconducting order parameter Δ is constant in the superconductor and zero in the normal metal.

II. CONDUCTANCE OF A LONG NORMAL SLAB ATTACHED TO A SUPERCONDUCTOR

A. Model

We consider a ballistic normal-metal or semiconductor slab between two normal reservoirs. The slab is separated by an infinite barrier from a region denoted as vacuum, except
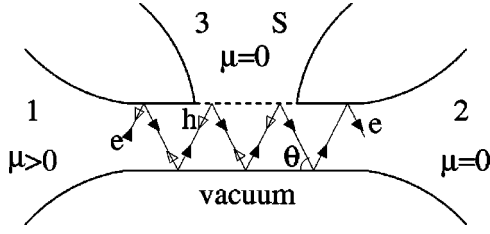
FIG. 1. Vacuum–ballistic normal-metal–superconductor junction with a barrier at the NS interface. Each time the particle hits the NS interface it can be reflected either normally or in an Andreev process. Here 1 and 2 are normal reservoirs and 3 is a superconducting reservoir. θ is the angle of incidence. Solid (open) arrows designate electrons (holes). In Sec. V a similar structure is considered, with a second superconductor attached to the other (lower) side of the slab, so the structure has up-down symmetry.

in a region of length L, at which a superconductor is attached to the slab (Fig. 1). At the NS interface the barrier is finite, with transmission probability Γ. The opening of the normal slab to the two normal reservoirs is taken to be adiabatic and the length of the slab between the reservoirs and the NS interface to be long enough such that channels are formed with homogeneous distribution in the transverse direction.[15] We also assume that the change from infinite barrier to finite barrier of transmission Γ at the end points of the NS interface is not abrupt, but smeared over a length s such that $\lambda_F \ll s \ll W$, where W is the width of the slab in the direction perpendicular to the interface. In this way the change is adiabatic but the smearing can be neglected in our calculations. We denote this structure as a vacuum–normal-metal–superconductor (VNS) structure, as opposed to a similar structure with another superconductor attached symmetrically to the other side of the slab, which will be denoted an SNS structure.

The superconductor is connected to a third reservoir except when explicitly mentioned otherwise. We consider the case where the electrochemical potentials of the right and superconducting reservoirs are equal, and the left reservoir is biased by an infinitesimal voltage, and calculate the three-terminal linear conductances of the system. Previous works concerning similar structures[16–19] considered the NS interface either as fully transparent or concentrated on effects of channel mixing due to the roughness of the barrier when it exists. We consider the NS interfaces to have a smooth barrier, so that normal reflection is specular and the Andreev reflected hole retraces the electron's trajectory. We assume specular reflection from the VN interface as well.

Our model is two dimensional. While assuming $\lambda_F \ll W$, therefore having many channels, we assume for simplicity that the thickness of the slab (the third dimension) is small, having one transverse mode in this direction. The generalization of our treatment to thicker slabs is trivial.

We use a semiclassical formalism and consider the propagation of electrons in each channel to be described by their classical deterministic trajectory.[3,20] For each channel j we define $k_{j\parallel} = \sqrt{2mE_F/\hbar^2 - j^2\pi^2/W^2}$ and calculate the angle $\theta_j = \tan^{-1}[j\pi/(k_{j\parallel}W)]$ between the classical trajectory of an electron in this channel and the NS interface. We consider an

electron entering the normal slab from the left reservoir, approaching the region of the slab with the NS interface ("NS region") at a given distance from the NS interface and angle θ_j with respect to it. If the electron is only normally reflected from the NS interface, it follows a certain trajectory in the slab until exiting it to the right reservoir after hitting the NS interface N times ("N trajectory"). Due to the finite Andreev reflection amplitude at each point it hits the NS interface, the electron has a probability $R_{he}(N)$ to be reflected as a hole to the left reservoir. In this model, due to the interfaces being parallel and smooth, there is zero probability for an electron to be reflected back to the left reservoir or to be transmitted as a hole to the right reservoir. Therefore, $R_{he}(N) + T_{ee}(N) = 1$, where $T_{ee}(N)$ is the probability of an electron coming from the left reservoir to be transmitted as an electron to the right reservoir.

For each open channel in the slab the number of times a trajectory hits the NS interface is either N_j or $N_j + 1$, where N_j equals the integer part of $L\tan\theta_j/(2W)$, with L being the length of the NS interface. The fraction of trajectories in channel j that hit the NS interface $N_j + 1$ times is given by $p_j = L\tan\theta_j/(2W) - N_j$. The Andreev reflection probability of an electron in channel j is then given by

$$R_{he}^j \equiv p_j R_{he}(N_j + 1) + (1 - p_j) R_{he}(N_j). \tag{1}$$

We define by I_1, I_2, and I_3 the currents emerging from the left terminal, right terminal, and superconducting terminal, respectively. Due to current conservation, $I_1 = -I_2 - I_3$. We then define the NN, NS, and total linear conductances of the system as

$$G_{21} \equiv -\lim_{V \to 0} \frac{I_2}{V} = \frac{2e^2}{h} \sum_j \Theta(k_{j\parallel}^2)(1 - R_{he}^j), \tag{2}$$

$$G_{31} \equiv -\lim_{V \to 0} \frac{I_3}{V} = \frac{4e^2}{h} \sum_j \Theta(k_{j\parallel}^2) R_{he}^j, \tag{3}$$

and

$$G_T \equiv \lim_{V \to 0} \frac{I_1}{V} = G_{21} + G_{31} = \frac{2e^2}{h} \sum_j \Theta(k_{j\parallel}^2)(1 + R_{he}^j), \tag{4}$$

where $\Theta(x)$ is the Heaviside theta function.

B. Andreev reflection probability of an N trajectory

The calculation of the conductances is therefore reduced to the calculation of $R_{he}(N) \equiv |r_{he}(N)|^2$ where $r_{he}(N)$ is the corresponding amplitude. For a single hit at the NS boundary, we denote by r_{he} (r_{eh}) the amplitude for an electron (hole) to be Andreev reflected and by r_{ee} (r_{hh}) the amplitude for an electron (hole) to be normally reflected. By dividing an N trajectory to an $N-1$ trajectory and a 1 trajectory, we obtain a recursion formula
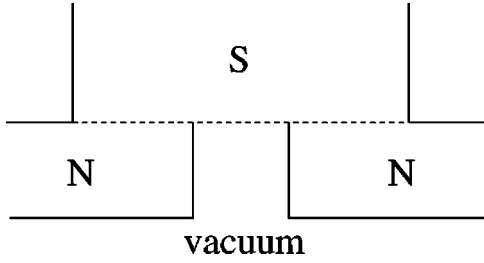
FIG. 2. Vacuum–ballistic normal-metal–superconductor junction where a part of the normal metal is removed (only the relevant region is shown).

$$r_{he}(N) = r_{he} + r_{ee}r_{he}(N-1)r_{hh}$$
$$+ r_{ee}r_{he}(N-1)r_{eh}r_{he}(N-1)r_{hh} + \cdots$$
$$= r_{he} + \frac{r_{ee}r_{he}(N-1)r_{hh}}{1 - r_{eh}r_{he}(N-1)}. \tag{5}$$

Using the relations (which are exact at E_F) $r_{ee} = r_{hh}^*$, $r_{eh} = r_{he}$, and $|r_{eh}|^2 + |r_{ee}|^2 = 1$, we assume, and then show by induction, that $r_{he}(N)$ is imaginary for all N and can be written as

$$r_{he}(N) = i \frac{|r_{he}(N-1)| + |r_{he}|}{1 + |r_{he}||r_{he}(N-1)|}. \tag{6}$$

The solution of this equation is given by

$$r_{he}(N) = i \tanh[N \tanh^{-1}(|r_{he}|)]. \tag{7}$$

For a barrier with small transmission probability we find

$$R_{he}(N) \approx \tanh^2(Nr) \approx \tanh^2(N\Gamma/2), \tag{8}$$

where we define $r \equiv |r_{he}| = \Gamma/(2-\Gamma)$.

Using Eq. (7) to obtain the values of $R_{he}(N)$ for all the channel-dependent N_j and N_j+1 in the conductance formulas [Eqs. (2)–(4)], we obtain the linear conductances G_{21}, G_{31}, and G_T. In this paper we are interested in the case where $\Gamma \ll 1$ and, therefore, in some of the formulas, and in the qualitative discussions, we take this limit.

Before considering further the conductances of the system, we would like to dwell on the physical aspects of Eq. (8). This formula reflects the essence of the physics behind "reflectionless tunneling." It states that electrons in trajectories that hit the NS interface $N \gg 1/\Gamma$ times are Andreev reflected with probability close to unity, even though $\Gamma \ll 1$, thus making a barrier having a low transmission coefficient effectively transparent to pair current. This is a result of electron-hole coherence in the normal metal. For an incoming electron, the different paths resulting in a hole returning to the reservoir interfere constructively, while the different paths resulting in an electron transmitted to the right reservoir interfere destructively. The constructive interference for a returned hole competes with the small Andreev amplitude at each encounter with the interface, which is proportional to Γ, and therefore $R_{he}(N) \approx 1$ only for $N \gg \Gamma^{-1}$. This means that for channels in which $\tan\theta \gg 2W/(\Gamma L)$ the barrier at the NS interface is not effective. In fact, if one considers a sys-

tem in which the superconductor is floating and the above condition is fulfilled for all the channels, one can show that the current between the left and right reservoirs flows inside the superconductor and a part from the middle of the normal slab can be taken out (see Fig. 2) without affecting the conductance of the system.

Equations (7) and (8) are far more general than the above model and hold in any case where an electron in the normal metal can hit the NS interface more than once before electron-hole coherence is lost. This is true in various geometries in ballistic systems, and also in diffusive systems, which are considered in Sec. VII. In all these cases, Eq. (8) results in a criterion for the effectiveness of a barrier with small transmission probability: *Consider a physical property which is determined by a certain set of trajectories; the criterion for the barrier at the NS interface not to be effective is that most of these trajectories hit the interface more than Γ^{-1} times before electron-hole coherence is lost.* In Sec. VII we will show how this general criterion reduces, in diffusive systems, to the known conditions for the barrier, though high ($\Gamma \ll 1$), not to affect the conductance and the density of states of a diffusive NIS junction.

C. Comparison to an incoherent structure

In order to show that Eq. (8) is a result of constructive interference, which is due to electron-hole coherence, we compare our result to the case where, due to strong dephasing, there is no electron-hole coherence, i.e., where the phase between two consecutive hits of the interface is lost. In this case the problem is reduced to a random walk problem, with forward-backward asymmetry. At each hit at the NS interface the electron (hole) has a probability $\Gamma^2 \ll 1$ to be Andreev reflected, in which case the direction of propagation is reversed and the probability to move forward is $1 - \Gamma^2$. The size of the step is channel dependent and is given by $d_j = 2W \cot\theta_j$, the distance between two consecutive points a trajectory in channel j hits the interface. This gives a mean free path of $l_j = d_j/\Gamma^2$. For $L \ll l_j$ the Andreev reflection probability is $R_{he} = L/l_j$, and for $L \gg l_j$ it is $1 - l_j/L$ (the probability for a transmitted electron is l_j/L). Therefore l_j is the saturation length, beyond which the Andreev reflection probability is close to unity. On the contrary, in the case of coherent scattering, using Eq. (8) and the relation $N_j = L/d_j$, we find that the saturation length is $d_j/\Gamma = l_j\Gamma$. Due to the scattering being coherent, it is smaller by Γ compared to the noncoherent case. Moreover, for short slabs, $L \ll l_j\Gamma$, $R_{he} \approx L^2/(4l_jd_j)$, larger by $L/(4d_j)$ than the non-coherent case. For long slabs ($L \gg l_j\Gamma$) one obtains $R_{he} \approx 1 - \exp(-L/\sqrt{2l_jd_j})$, and the probability for a transmitted electron is exponentially small, and not linear in l_j/L as in the noncoherent case. The difference between the two cases is most notable for slabs with intermediate lengths between the two saturation lengths, $l_j\Gamma \ll L \ll l_j$, which corresponds to $1/\Gamma \ll N \ll 1/\Gamma^2$. Without coherence $R_{he} \ll 1$, and with coherence $R_{he} \approx 1$.

It is instructive to compare Eq. (8) to a similar system, in which the superconductor is not attached to the slab on its side, but part of the slab itself, of length L, is superconduct-
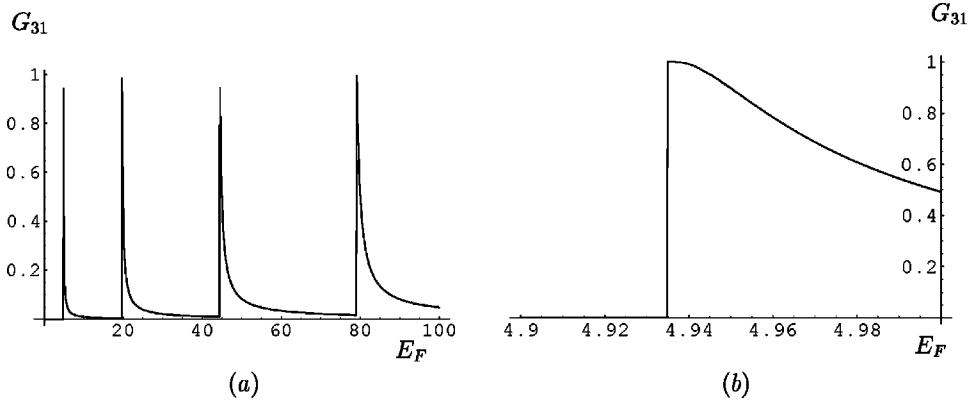
FIG. 3. (a) The conductance (in units of $4e^2/h$) between the left normal reservoir and the superconductor is plotted as function of E_F [in units of $\hbar^2/(mW^2)$] for $L\Gamma/(4W)=0.1$. (b) Enlarging the first peak we see that the conductance at the peak is unity, and the width of the peak is approximately $[L\Gamma/(4W)]^2=0.01$ of the value of E_F at the peak.

ing. In this case and assuming no barrier at the NS interfaces, the Andreev reflection probability of an incoming electron is given by $\tanh^2(\Delta L/2\hbar v_F)\equiv\tanh^2(L/2\xi_s)$.[21] Here it is ξ_s, the ballistic superconducting coherence length, which is the length scale for pairing. In our system, Eq. (8) can be written as

$$R_{he}(L)\approx\tanh^2[L\Gamma/(2d_j)], \qquad (9)$$

with the saturation length d_j/Γ as the length scale for pairing in the normal slab due to the proximity to the attached superconductor.

III. CHANNEL OPENING

Using Eqs. (3) and (7) the NS linear conductance can be calculated as function of E_F, Γ, L, and W. We now concentrate on a special case of these parameters, which results in sharp resonances of the NS linear conductance as a function of the Fermi energy. While in all the other cases considered in this paper we are interested in the emergence of constructive interference that leads to enhanced Andreev reflection and therefore consider cases in which electrons in at least some of the channels hit the interface $N\gg1/\Gamma$ times, we are now interested in a different limit, in which $\Gamma L\sqrt{k_F/W}\ll1$. The generic behavior in such a structure would be that the current flow to the superconductor is small, since the number of times an electron in any transverse channel hits the barrier is smaller than $1/\Gamma$. However, if we change the Fermi energy (e.g., by a back gate) such that the channel of the highest transverse mode has just opened, then the trajectory of a particle in this channel is almost perpendicular to the interface. As a result, the number of times a particle in this channel hits the interface is much larger than $1/\Gamma$ and the contribution of this channel to the NS conductance is significant and given by

$$G_{31}^{sing}=\frac{4e^2}{h}\Theta(k_{j\parallel}^2)\tanh^2\frac{j\pi L\Gamma}{4W^2k_{j\parallel}}. \qquad (10)$$

In this equation we assumed that $\Gamma\ll1$ and neglected the fact that a fraction of the trajectories hit the barrier N_j+1 and not

N_j times, since as the channel opens $N_j\gg1$. Defining $\epsilon_j=\hbar^2(k_{j\parallel})^2/(2m)$ and $\widetilde{\epsilon}=[L\Gamma/(4W)]^2E_F$ we find that for $0<\epsilon_j\ll\widetilde{\epsilon}$

$$G_{31}^{sing}=\frac{4e^2}{h}\tanh^2\sqrt{\frac{\widetilde{\epsilon}}{\epsilon_j}}\approx\frac{4e^2}{h}[1-4e^{-2\sqrt{\widetilde{\epsilon}/\epsilon_j}}]. \qquad (11)$$

While in a normal quantum point contact connected to a superconductor in series the linear NS conductance as function of the Fermi energy in the slab would show steps,[22] in our case, where a superconductor is attached to the point contact on its side, with a barrier at the interface, the NS conductance as a function of E_F has sharp *peaks* at the energies where channels open. The magnitude of these peaks is 4 times the quantum conductance, and the scale of their energy width is $\widetilde{\epsilon}$. With the condition given above, $\Gamma L\sqrt{k_F/W}\ll1$, these peaks are narrower than the energy difference between the opening of adjacent channels. For $L\approx W$ this condition reduces to $\Gamma\ll\sqrt{\lambda_F/W}$. Under the semiclassical approximation we make the conductance peaks are nonanalytical as a function of Fermi energy at energies where transverse channels are opened, as can be seen both in Eq. (11) and Fig. 3. This is due to the fact that the number of times an electron hits the interface diverges as $\epsilon_j\to0$. These nonanalyticities are a consequence of the semiclassical model, and one has to take into account that the validity of the semiclassical approximation is limited by the condition $k_{j\parallel}\gg1/L^*$, where L^* is the range of the potential variation. We estimate L^* by $k_\perp/\nabla k_\perp=W*s/(\lambda_F\sqrt{\Gamma})$, taking into account the variation of $k_\perp$ with the spatial variation of Γ. The condition $k_{j\parallel}\gg1/L^*$ is equivalent to $\epsilon_j\gg[\Gamma\lambda_F^4/(W^2s^2)]E_F$, which is consistent with the condition $\epsilon_j\ll\widetilde{\epsilon}$ given that $\Gamma\gg\lambda_F^4/(L^2s^2)$. One can therefore expect that with this condition fulfilled, going beyond the semiclassical approximation would smoothen the above nonanalyticities, but will not alter the other features of the peaks (height and width). For $\epsilon_j\gg\widetilde{\epsilon}$ the contribution of the jth channel to the NS conductance is proportional to $1/\epsilon_j$ and is given by
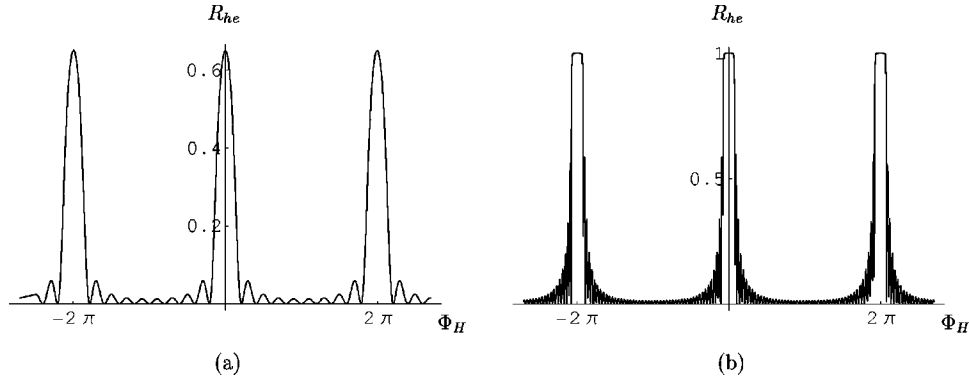
FIG. 4. $R_{he}(N, \Phi_H)$ as obtained from Eq. (17) for (a) $N=10$ trajectory and (b) $N=50$ trajectory in a VNS system (Fig. 1) for a barrier transmission probability $\Gamma = 0.2$. Notice the narrow large peaks periodic in Φ_H and the small oscillations between each such peaks, having in (a) $N-1=9$ nodes. In (b) the magnitude at the high peaks is approximately unity, and the oscillations between them are hardly visible.

$$G_{31}^j = \frac{4e^2}{h} \frac{\tilde{\epsilon}}{\epsilon_j}. \qquad (12)$$

In this section we described the effect of channel opening on the NS conductance of the system. The behavior of G_T is similar, only the peaks at the energies where channels open are half the magnitude and are on top of the step function of magnitude $2e^2/h$ (since G_T is similar to G_{31}, only $2R_{he}^j$ is replaced by $1 + R_{he}^j$). The NN conductance is given by the complementary of half the NS conductance to a step function ($2R_{he}^j$ is replaced by $1 - R_{he}^j$). In the next sections we mostly consider G_{31}, and analogies to G_T and G_{21} can be made in a similar way.

IV. MAGNETOCONDUCTANCE OF A LONG NORMAL SLAB ATTACHED TO A SUPERCONDUCTOR

In this section we consider the same VNS structure as in Secs. II and III with a magnetic field applied perpendicular to the slab. We investigate the effect of the magnetic field on the transmission probability of an N trajectory, as well as on the linear conductances in the system. Magnetic field penetration into the superconductor is neglected.

We consider $H \ll \Phi_0/(\lambda_F^{1/2} W^{3/2})$ where Φ_0 is the flux quantum. Under this condition the curving of the trajectories of the particles in the normal slab can be neglected.[23] The number of times, N_j (or $N_j + 1$), a trajectory of an electron in channel j hits the NS interface stays unchanged, and so do Eqs. (2)–(4), except that the Andreev reflection probabilities $R_{he}(N)$ now depend also on Φ_H, the phase acquired by an electron and a hole moving in opposite directions between two consecutive points the trajectory hits the NS interface ("trajectory section"). This phase is given by $\Phi_H = 4\pi H A/\Phi_0$, where A is the area of the triangle enclosed by the trajectory section and the interface.

We now turn to the calculation of $R_{he}(N, \Phi_H)$. Repeating the same procedure leading to Eq. (5), but keeping track of the phase introduced by the magnetic field, we obtain

$$r_{he}(N, \Phi_H) = r_{he} + \frac{r_{ee}r_{he}(N-1, \Phi_H)e^{i\Phi_H}r_{hh}}{1 - r_{eh}r_{he}(N-1, \Phi_H)e^{i\Phi_H}}. \qquad (13)$$

In order to obtain an explicit formula for $r_{he}(N, \Phi_H)$ it is useful to define

$$r_{he}(N, \Phi_H) = r_{he} \frac{\beta_N}{\gamma_N}, \qquad (14)$$

where β_N and γ_N are also Φ_H dependent. Inserting this definition for N and $N-1$ into Eq. (13) we obtain the matrix equation

$$\begin{pmatrix} \beta_N \\ \gamma_N \end{pmatrix} = \begin{pmatrix} e^{i\Phi_H} & 1 \\ r^2 e^{i\Phi_H} & 1 \end{pmatrix} \begin{pmatrix} \beta_{N-1} \\ \gamma_{N-1} \end{pmatrix} = \begin{pmatrix} e^{i\Phi_H} & 1 \\ r^2 e^{i\Phi_H} & 1 \end{pmatrix}^{N-1} \begin{pmatrix} 1 \\ 1 \end{pmatrix}. \qquad (15)$$

Here we used the fact that at the Fermi energy r_{he} is imaginary. β_N and γ_N are in principal defined up to (the same) multiplication constant, which we dictate by the choice $\beta_1 = \gamma_1 = 1$. Diagonalizing the matrix and taking it to the power $N-1$ we obtain

$$r_{he}(N, \Phi_H)$$

$$= \frac{ire^{-i\Phi_H/2}}{-i\sin(\Phi_H/2) + \sqrt{b}\coth\left[N\tanh^{-1}\left(\frac{\sqrt{b}}{\cos(\Phi_H/2)}\right)\right]}, \qquad (16)$$

where $b = r^2 - \sin^2(\Phi_H/2)$. Using the fact that the second term in the denominator is always real (also when b is negative) we obtain

$$R_{he}(N, \Phi_H) = \frac{r^2}{\sin^2(\Phi_H/2) + b\coth^2\left[N\tanh^{-1}\left(\frac{\sqrt{b}}{\cos(\Phi_H/2)}\right)\right]}, \qquad (17)$$
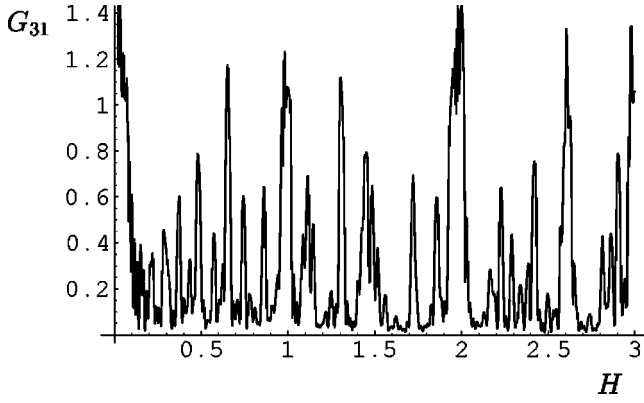
which, for $b < 0$, can be written as

FIG. 5. The conductance (in units of $4e^2/h$) between the left normal reservoir and the superconductor as a function of H (in units of Φ_0/W^2). The plot is given for $L/W=50$, $\Gamma=0.1$, and $2mE_FW^2/\hbar^2=1000$, which corresponds to ten open channels. Peaks higher than unity are a result of overlapping resonances of two or more channels. Apparent periods of H are 0.29, 0.37, 0.48, and 0.65. At $H=0$ the peak is significantly higher than the others ($G_{31}=5$, not shown).

$$R_{he}(N,\Phi_H)=\frac{r^2}{\sin^2(\Phi_H/2)+(-b)\cot^2\left[N\tan^{-1}\left(\frac{\sqrt{-b}}{\cos(\Phi_H/2)}\right)\right]}. \tag{18}$$

These formulas hold for any N, $r(\Gamma)$, and H. We now consider the case of $r\ll1$ and $Nr\gg1$. For $\sin^2(\Phi_H/2)\gg r^2$ (which holds for most values of Φ_H when $r\ll1$), we see from Eq. (18) that $R_{he}(N,\Phi_H)\ll1$. In the opposite limit, of $\sin^2(\Phi_H/2)\ll r^2$, one obtains from Eq. (17) that $R_{he}(N,\Phi_H)\approx1$. This leads to the conclusion that the Andreev reflection probability from an N trajectory is small for almost all values of perpendicular magnetic field, except those special values that result in $|\Phi_H-2k\pi|\lesssim r$ (Fig. 4). Between every two such peaks the function oscillates, having $N-2$ smaller peaks (and $N-1$ nodes). These peaks (nodes) correspond to integer (half integer) flux quanta through an area of an integer number of triangles in the trajectory of the specific channel.

The magnetic field not only impairs the constructive interference leading to large Andreev reflection at zero field, but causes destructive interference. This can be seen by considering $\Phi_H=\Phi_0/2$. Then, $R_{he}(N)=0$ for even N and for odd N it equals r^2, the Andreev reflection probability from a single hit. Therefore, for any given channel R_{he}^j is of order r^2. In the cases discussed in Sec. II C, of no interference and of constructive interference, there were (different) saturation lengths beyond which the Andreev reflection probability was close to unity. Here, however, due to destructive interference, there is no such length scale and Andreev reflection is small (r^2) *for any length of NS interface*. This is true also when the destructive interference is due to a superconducting phase difference in an SNS structure, as is discussed in Sec. V.

Inserting Eq. (17) in the conductance formulas [Eqs. (2)–(4)] we obtain the linear conductances as function of mag-

netic field for any junction parameters (Γ,L,W,E_F). If the parameters of the structure are such that $\Gamma L/W\gg1$, then at zero magnetic field the NS dimensionless conductance is much larger than unity, since there are many channels for which $N\Gamma\gg1$. We choose such a case and plot in Fig. 5 the NS dimensionless conductance as a function of H. At $H=0$ the conductance has a sharp peak, of magnitude of the order of the number of channels and width of order r. As H is increased, the constructive interference leading to the enhanced Andreev reflection is destroyed in one channel after the other and the NS conductance becomes small. However, the conductance of each channel is periodic in H, with a period given by the area of the triangle between a trajectory section in this channel and the interface. This quasiperiodicity is reflected in the peak spectrum of the NS conductance as function of H (Fig. 5). Periods of larger H reflect channels with a smaller triangle, which corresponds to a trajectory of larger N, and therefore [see Eq. (8)] the peak heights are larger. Using this quasiperiodicity one can obtain "magnetic switching." By choosing the magnetic field such that $|\Phi_H^j=2k\pi|$ for one channel only, one can remove only electrons propagating in this channel from the normal slab to the superconductor and have the electrons in all the other channels propagate to the right reservoir with probability close to unity.

Though the results in this section were given for the linear conductance at finite magnetic field, it is straightforward to generalize our results to be valid for finite subgap voltage, thus obtaining the differential conductance as a function of voltage. One can also incorporate a constant phase gradient $\nabla\phi$ in the superconductor in parallel to the NS interface, generated by a constant supercurrent. The Andreev reflection amplitude from an N trajectory would then be given by Eq. (16) with Φ_H replaced by

$$\Phi_{tr}=\Phi_H+\nabla\phi d_j+\Phi_j^{tr}(\epsilon). \tag{19}$$

Here $\Phi_j^{tr}(\epsilon)=(k_{j\parallel}^+-k_{j\parallel}^-)W/\sin\theta_j+\arg[r_{ee}r_{hh}]$ is the relative electron-hole phase accumulated due to finite energy in one triangle, where $k_{j\parallel}^\pm=k_{j\parallel}(E_F\to E_F\pm\epsilon)$. Note that there is a complete analogy between applying a perpendicular magnetic field and constant gradient of the superconducting phase, with the relation $\nabla\Phi=2\pi HW/\Phi_0$. For $H=0$ and $\nabla\Phi=0$, we obtain a zero-bias peak in the differential NS conductance as a function of voltage, similar to the low-H behavior of the NS conductance as shown in Fig. 5.

V. CONDUCTANCE PARALLEL TO THE INTERFACE IN AN SNS SYSTEM

We now consider a system in which a second superconductor is attached symmetrically to the other side of the slab, so the structure has up-down symmetry. We consider the case in which the two barriers between the normal slab and the superconductors have the same transmission probability Γ. Then, one can apply the same approach we used in the previous sections, only count the number of hits of each trajectory at both interfaces. The calculation of $R_{he}(N,\Phi_s)$ is given in Appendix A. It is done in the same spirit as the
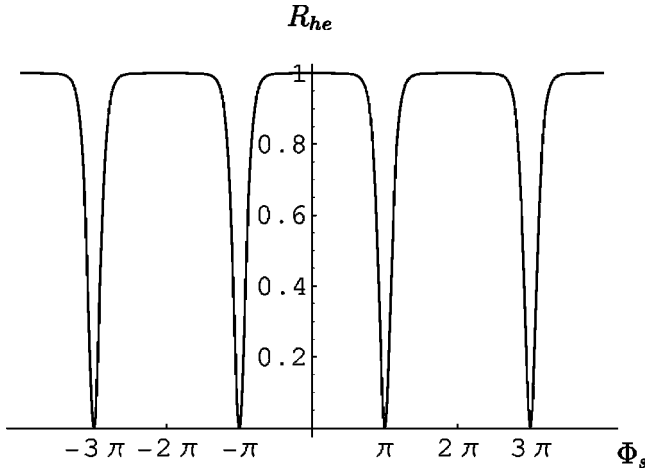
R_{he}

FIG. 6. $R_{he}(N,\Phi_s)$ in an SNS structure for $N=50$ and $\Gamma=0.2$. Note the narrow dips, in comparison to the narrow peaks in Fig. 4(b), which is drawn for the same N and Γ, as a function of H.

calculation of $R_{he}(N,\Phi_H)$, but is more elaborate since one has to distinguish between even and odd times a trajectory hits the interface, and the recursion relations are more complicated. The result for even N is

$$R_{he}(2N,\Phi_s)$$

$$=\left\{z+(1-z)\right.$$

$$\left.\times\coth^2\left[N\tanh^{-1}\left(\frac{2r\cos(\Phi_s/2)\sqrt{(1-z)}}{1+r^2\cos\Phi_s}\right)\right]\right\}^{-1} \quad (20)$$

where $z=r^2\sin^2(\Phi_s/2)$. The result for odd N is similar and is given in Appendix A. These results are even in Φ_s and, therefore, the same for a trajectory hitting first either of the two superconductors. For $r\ll 1$ we obtain $R_{he}(2N,\Phi_s)=\tanh^2[2Nr\cos(\Phi_s/2)]$. For $Nr\gg 1$ we see that $R_{he}(2N,\Phi_s)\approx 1$ unless $|\Phi_s-(2k+1)\pi|\lesssim\pi/(Nr)$, while $R_{he}(2N,\Phi_s)=0$ for $\Phi_s=(2k+1)\pi$. As a result, in this limit, the Andreev reflection probability from a $2N$ trajectory as a function of Φ_s has sharp *dips* near $\Phi_s=(2k+1)\pi$ of an approximate width of $1/(2Nr)$ (Fig. 6). The transmission probability of electrons to the right reservoir is given by $1-R_{he}(2N,\Phi_s)$ and has sharp resonant peaks, which indicates that there is a transverse Andreev level shifted to E_F at $\Phi_s=(2k+1)\pi$, similar to the case in standard SNS junctions.[24] As in the case of perpendicular magnetic field, $R_{he}(2N,\Phi_s)$ has a maximum at $\Phi_s=0$ (or multiples of 2π), but there are two major differences between the dependence of $R_{he}(N)$ on H and on Φ_s: (i) In a period of $2\pi R_{he}(N,\Phi_s)$ has one minima, where $R_{he}(N,\Phi_H)$ has N minima. (ii) while $R_{he}(N,\Phi_H)$ exhibits sharp *peaks* near $\Phi_H=2\pi n$, and for most values of magnetic field (generically) constructive interference is lost, and Andreev reflection is small, the situation for $R_{he}(N,\Phi_s)$ is opposite. It is close to unity for most values of phase difference, and exhibits sharp *dips* near $\Phi_s=\pi+2\pi k$.
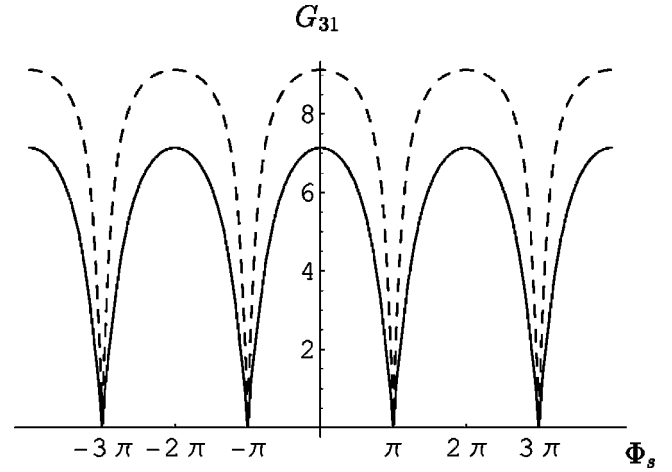
G_{31}

FIG. 7. G_{31} (in units of $4e^2/h$) as a function of Φ_s. The solid curve is given for the same parameters as in Fig. 5 to enable comparison. In contrast with the case of applied magnetic field, the conductance is periodic in Φ_s, has narrow dips at odd multiples of π, and the oscillations as a function of Φ_s are of the order of the full conductance (giant). The dashed line is plotted for the same parameters, except here $\Gamma=0.25$. The larger conductance and the narrower dips are both a result of $N\Gamma$ being larger for each channel.

These differences can be understood by examining the two mechanisms of the destruction of the constructive interference between different paths of the same trajectory that result in a hole returning to the left reservoir. Indeed, the phase difference between a hole resulting from an Andreev reflection at the first hit of the NS interface and a hole resulting from an Andreev reflection at the second hit of the NS interface is similar in both cases (Φ_H and Φ_s), but the phase difference between this hole and a hole resulting from an Andreev reflection at the Nth hit of the NS interface is very different for the two cases. It is $(N-1)\Phi_H$ for the case of a magnetic field and Φ_s or 0 (depending if N is even or odd) for the case of superconducting phase difference. This introduces a large amplification factor in the electron-hole phase difference introduced by the magnetic field compared to that introduced by the superconducting phase difference. As a result, the magnetic field is far more efficient in destroying the constructive interference leading to the enhanced Andreev reflection.

The linear conductances as function of Φ_s are calculated by inserting the results for the Andreev reflection probabilities [Eqs. (20) and (A10)] in the conductance formulas [Eqs. (2)–(4)]. N_j in the VNS structure is now replaced by $\hat{N}_j$ which equals the integer part of $L\tan\theta_j/W$ and p_j is replaced by $\hat{p}_j=L\tan\theta_j/W-\hat{N}_j$. In Fig. 7 we plot (solid line) the NS conductance as a function of the superconducting phase difference for a system with the same parameters as the one in Fig. 5, for comparison. The NS conductance for a similar structure with a larger barrier transmission probability ($\Gamma=0.25$) is also plotted (dashed line) to demonstrate the narrowing of the width of the dips as $N\Gamma$ grows. Here we see another marked difference between applying a perpendicular magnetic field in the VNS structure and a phase difference in the SNS structure. In the case of the applied magnetic field
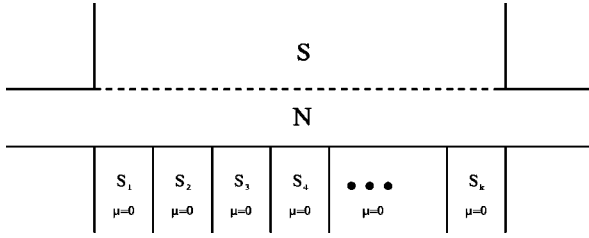
FIG. 8. SNS junction where the bottom superconductor is divided to pieces with controllable phase of the order parameter (only the relevant region is shown).

there is a large peak at $H=0$, to which all the channels contribute due to the constructive interference, but the periodic peaks at higher fields appear for each channel at a different H. If the parameters of the junction are such that the separations between conductance peaks are smaller than their width, the result will be a smooth oscillatory behavior of the conductance as function of H. On the other hand, in the case of SNS structure, the dips at all $\Phi_s=(2k+1)\pi$ are common to all the channels, and therefore the conductance oscillations as a function of Φ_s show sharp features of magnitude of the order of the total conductance.

Recently, Petrashov *et al.* measured large conductance oscillations as a function of the magnetic field and superconducting phase difference in a normal slab connected to "superconducting mirrors."[25,26] Our results cannot be directly applied to the experimental structures studied by Petrashov *et al.*, since in the experiment the structures are different, the superconductor is floating, and there is finite scattering in the normal slab. However, some features appear to be more general and exist both in the experimental results and in our calculations. These are the much larger magnitude and sharpness of the oscillations as a function of superconducting phase difference compared to the oscillations as a function of magnetic field.

To conclude this section we now apply the results obtained above to show how one can get controlled current withdrawal from an electronic waveguide. Here we use the fact that as long as the phase difference between the superconductors is π, the electrons move in the slab as in a waveguide. By replacing the bottom superconductor with a series of superconductors (Fig. 8), each with a controllable phase ϕ_i and interface length with the slab, $\tilde{L}$, we can create a "switch" in which we can control the location where the current is drawn. We set $\phi_{i\neq\tilde{i}}=\pi$ and $\phi_{\tilde{i}}=0$. For all $i\neq\tilde{i}$ an incoming electron from the left in an angle with $\tan\theta \gg (2W/\tilde{L}\Gamma)$ will be normally reflected as in a waveguide. However, when it reaches the $\tilde{i}$th superconductor Andreev reflection occurs, adding a Cooper pair to the superconductor. One can therefore inject a current from the left reservoir and draw it at any one of the superconducting slabs.

VI. SHOT NOISE

In this section we calculate the shot noise as a function of H in the VNS structure and Φ_s in the SNS structure, and show that the differences between applying magnetic field
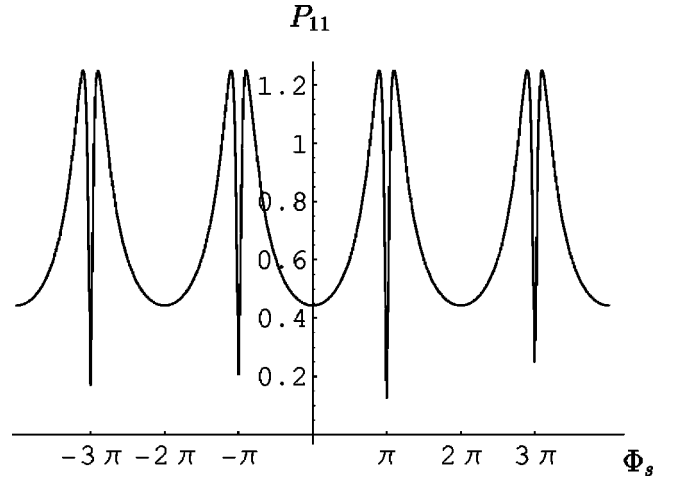

FIG. 9. P_{11} in units of P_0 as a function of Φ_s for the geometry where the normal slab is attached to two superconductors. The parameters of the system are the same as those in Fig. 7 (dashed line).

and superconducting phase difference are reflected remarkably in the shot noise properties of the systems.

We define the quantities $P_{ll'}=2\int_{-\infty}^{\infty}dt\langle\Delta\hat{I}_l(t)\Delta\hat{I}_{l'}(0)\rangle$ (where l,l' are normal terminal indices), which give both the shot noise and the cross correlators between current fluctuations at the two normal terminals. Anantram and Datta[27] considered the case where an arbitrary number of superconducting and normal terminals exist, with the restriction that the chemical potential in all the superconducting terminals is the same, and obtained general equations for the current correlators. Using their equations for our system we obtain

$$P_{11}=P_{22}=P_{12}=P_0\sum_j \Theta(k_{j\parallel}^2)R_{he}^j(1-R_{he}^j), \quad (21)$$

where $P_0=2e|V|(2e^2/h)$. This formula is applicable for both the VNS and SNS structures, and the specific parameters of the junction as well as the H and Φ_s dependence enter only into R_{he}^j. Notice the full positive noise correlations between the two normal terminals,[28] which is a result of zero normal reflection to the same reservoir and Andreev transmission to the other reservoir in our model.

Due to the dependence of the shot noise on the functions $R_{he}^j(1-R_{he}^j)$, it shows peaks at points where the Andreev reflection amplitude is neither close to zero or unity. For the SNS structure we consider, this results in a sharp feature near the values of Φ_s corresponding to *dips* in the NS conductance $[\Phi_s=(2k+1)\pi]$, which are common to all the channels. The form of the sharp feature is two double peaks separated by a very sharp dip,[29] as can be seen in Fig. 9. As function of H, in the case of one channel, a sharp feature appears near each value of H corresponding to a *peak* in the conductance. However, these points are channel dependent, and as was the case for the conductance, the presence of many channels smears the sharp features as a function of H.

Our results for the noise are easily generalized to finite subgap energy (differential shot noise as a function of bias voltage) and gradient of the superconductor phase in the same manner discussed at the end of Sec. IV.
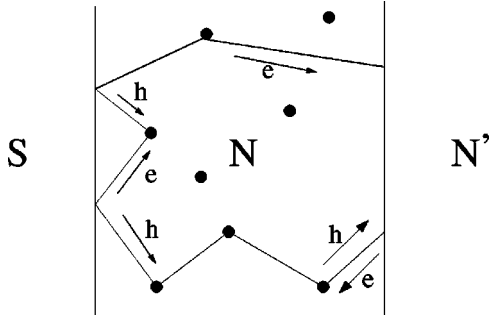
FIG. 10. Geometry of the model (Ref. 3), an example of a trajectory with $N=2$.

VII. DIFFUSIVE NS JUNCTIONS

The semiclassical approach, introduced by van Wees et al. to explain the phenomenon of reflectionless tunneling in diffusive NS junctions,[3] was used to analyze numerically other experimental results as well (see, e.g., Refs. 8 and 9). This approach has proved useful in obtaining a qualitative understanding of the physical phenomena in various geometries which make use of the standard methods (quasiclassical formalism, BdG equations) difficult. As Eq. (8) applies to any NS system, ballistic or diffusive, it can be used to obtain analytical results within this approach. In this section we apply the semiclassical formalism to treat both the phenomenon of reflectionless tunneling and the reduction of the local density of states (DOS) across a diffusive NS junction. We show that both of these phenomena are a result of the large transparency of the barrier to pair current (although $\Gamma \ll 1$ and under the conditions given by the general criterion at the end of Sec. II B) and thus stem from the same physical effect. We also demonstrate the connection between the effect of reflectionless tunneling in ballistic systems discussed in this paper, to the one in diffusive systems.

Since we consider the particle's trajectory in the normal metal to be deterministic, our approach can be expected to give correct quantitative results [Eqs. (22) and (23)] when the scattering potential varies slowly on a scale of a wavelength[3,30] and the sample is short enough such that classical dynamics will not develop phase space structures on scales smaller than $\hbar$.[31] For short-range disorder, this approach is expected to give results which are qualitatively correct.[3]

Following the treatment of Ref. 3, but using our analytical result for the Andreev reflection probability from an N trajectory, Eq. (7), we obtain the linear conductance of a normal slab connected via a barrier to a superconducting reservoir (see Fig. 10), which for $\Gamma \ll 1$ is given by

$$G(V \to 0, H = 0) = \frac{4e^2 n}{h} \sum_{N=0}^{\infty} T^2 (1-T)^{N-1} \tanh^2(N\Gamma/2).$$

(22)

Here n is the number of channels and T is the average transmission probability of the normal slab (the mean free path divided by its length). In the two limits where $\Gamma \ll T$ and $\Gamma \gg T$ Eq. (22) reduces to

$$G(V \to 0, H = 0) = \begin{cases} \dfrac{2e^2 n}{h} \dfrac{\Gamma^2}{T} & (\Gamma \ll T), \\[3mm] \dfrac{2e^2 n}{h} \left(\dfrac{1}{2T} + \dfrac{1}{\Gamma} \right)^{-1} & (\Gamma \gg T). \end{cases}$$

(23)

Unlike ballistic systems, in this case multiple reflections from the interface are enabled by the disorder. For small disorder $\Gamma \ll T$, the conductance is proportional to Γ^2, reflecting the fact that Andreev reflection is a two-particle process. Already in this limit the disorder increases the conductance by a factor of $1/T$. For $T \ll \Gamma$ the disorder is large enough to generate, with high probability, trajectories with $N \gg 1/\Gamma$, as we show below, and therefore the barrier is not effective and the conductance is linear in T. The conductance has a maximum for $T \approx \Gamma$, where $G \approx (2e^2 n/h)\Gamma \approx (2e^2 n/h)T$.

Equation (23) differs in the $\Gamma \gg T, T \to 0$ limit by a factor of 2 from the analogous formula obtained by Beenakker et al.[32] for short-range disorder. A detailed discussion of how this discrepancy results from the different assumptions in the two models is given in Appendix B.

As the essence of the effect of reflectionless tunneling is the fact that the barrier, though high, is transparent to pair current, the condition for the barrier to be ineffective was discussed for this phenomenon[33,34] as well as for other phenomena, as the reduction of the DOS on the normal side of an N-insulator-S (NIS) semi-infinite junction.[33] We now show, using random walk theory, that the criterion stated in Sec. II B, for the barrier to be ineffective, can be reduced in the diffusive case to the different known conditions for each phenomenon.

In Appendix C it is shown that the typical length of a diffusive trajectory between N consecutive times it hits the barrier is $L_N \approx N^2 l_n$, where l_n is the elastic mean free path in the normal metal (interestingly, there is no average length for an N trajectory; see Appendix C). This is also the order of magnitude of the length of the longest loop in such a trajectory (a loop is a part of a trajectory between two consecutive points it hits the interface). Using this result for L_N and since large contributions to Andreev reflection arise from trajectories that hit the interface $N \gg \Gamma^{-1}$ times before losing electron-hole coherence (8), only when coherent trajectories with total lengths larger than $L_\Gamma \equiv l_n/\Gamma^2$ occur with high probability will the barrier not be effective. This requires the electrons and holes to be coherent over a distance $\sqrt{L_\Gamma * l_n} = l_n/\Gamma$ from the interface. Therefore, the general condition in diffusive systems for the barrier to be ineffective is $\xi \gg l_n/\Gamma$, where ξ is the distance from the interface at which electrons and holes are still coherent. The coherence distance ξ is determined by the length of the slab, energy of the electron, or magnetic field, depending on the physical case considered. When measuring the conductance of an NS junction, then for zero energy and zero magnetic field, the length of the normal metal, d, is what limits the trajectories to lengths of order d^2/l_n (since a particle that reaches a distance d from the interface enters the reservoir, where phase coherence is lost). Therefore, the barrier is not effective when $\Gamma \gg l_n/d$.

Since the transmission probability through the diffusive normal part is roughly $T \approx l_n/d$, this condition reduces to the known condition[33] for the barrier to be ineffective, $\Gamma \gg T$ [in accordance with Eqs. (22) and (23)].

Following the same considerations one can obtain the condition for the barrier to be ineffective in various cases, noting the different mechanism impairing electron-hole coherence in each case. We consider, for example, the local DOS in a semi-infinite NS junction. The reduction of the local DOS in the normal side of an NS interface is closely related to the averaged amplitude of an electron near the interface to return to the same point as a hole through the pair amplitude $\langle \psi_\downarrow \psi_\uparrow \rangle$.[23] At zero energy and assuming the normal metal is semi-infinite, there is no mechanism that limits the length of coherent trajectories. The electron hits the barrier as many times as needed, $N \gg \Gamma^{-1}$, without losing electron-hole phase coherence, and according to Eq. (8), it is finally Andreev reflected. This results in a finite pair amplitude throughout the normal part, even in the presence of a barrier (at $\epsilon = 0$ there is no reduction of the pair amplitude due to phase averaging), and in a zero DOS at zero energy.

At finite energy ϵ, the electron and hole moving in opposite directions in a trajectory of length L accumulate a relative phase of $L\epsilon/(\hbar v_F)$, which limits the length of coherent trajectories to order $\hbar v_F/\epsilon$ and to distance $\xi = \xi_n \equiv \sqrt{\hbar D_n/\epsilon}$ from the interface (trajectories that traverse a distance longer than ξ_n result in phase difference of order 2π). The condition for having a large Andreev reflection amplitude is therefore $\Gamma \gg l_n/\xi_n$.[33] This condition assures that the total phase accumulated by the ingoing electron and outgoing hole is less than 2π, and therefore the averaging in $\langle \psi_\downarrow \psi_\uparrow \rangle$ results in finite pair amplitude and the local DOS is reduced. Similar considerations result in the width of the zero-bias anomaly in reflectionless tunneling being proportional to the Thouless energy.[23]

VIII. CONCLUSIONS

We have demonstrated the effect of reflectionless tunneling in a ballistic NS system in which the multiple reflections from the interface are due to the geometry. We considered a normal slab with superconductors attached to its sides, so the normal current flows in parallel to the NS interface. The barrier at the NS interface was taken to be smooth, so that normal reflection is specular, and with transmission probability $\Gamma \ll 1$. We obtained a formula for the Andreev reflection amplitude from a trajectory that hits the barrier at the NS interface N times and showed that, when $N \gg \Gamma^{-1}$, the barrier is transparent to pair current (though $\Gamma \ll 1$), leading to good proximity.

We have shown that having a smooth rather than rough barrier at the interface is advantageous in giving rise to more pronounced and delicate features, which are not averaged over. This results in new measurable phenomena, such as the sharp *peaks* in the NS conductance as new channels open (in contrast to the usual step function) and quasiperiodicity of the conductance as a function of magnetic field H. The smoothness of the barrier also enables one to conduct detailed manipulations such as extracting out a single channel

from a normal metal (semiconductor) waveguide or extracting the current at a given position along the waveguide.

By obtaining explicit formulas for the three-terminal conductances of the system as a function of H and of the superconducting phase difference Φ_s, we have shown that both H and Φ_s impair the constructive interference leading to the enhanced NS conductance, but in a qualitative different way. While as a function of H the enhanced NS conductance is limited to a small range of magnetic field and is channel specific, as a function of Φ_s the enhanced NS conductance is generic and is destroyed only near specific values of Φ_s (odd multiples of π) for all the channels, leading to giant conductance oscillations. This difference is also reflected clearly in the shot noise behavior as a function of both quantities.

By demonstrating the possibility to obtain large Andreev reflection in clean semiconductor-superconductor interfaces and the new possibilities such structures open, we hope to encourage experimental work in this regime.

Our results were obtained using a semiclassical formalism, with which we reduced a two-dimensional nonseparable problem to an effective one-dimensional problem. We have demonstrated the usefulness of this formalism in a few situations, and hopefully it can be used in the future to solve other problems which are hard to tackle using the conventional techniques.

We used this approach also for diffusive NS systems and demonstrated the connection between the effects of reflectionless tunneling in ballistic and diffusive NS junctions. We then considered the phenomena of reflectionless tunneling and the reduction in the density of states in diffusive NS junctions and showed that both can be obtained from a general criterion for the barrier, though large, to be transparent to pair current.

APPENDIX A: ANDREEV REFLECTION FROM AN N TRAJECTORY IN SNS JUNCTIONS

In this appendix we describe the recursion formalism leading to Eq. (20) and obtain a similar equation for trajectories that hit the NS interfaces an odd number of times.

We choose the phase of the upper superconductor to be $\Phi_s/2$ and the phase of the lower superconductor to be $-\Phi_s/2$. The Andreev reflection amplitude of an electron hitting the upper (lower) boundary is

$$r_{he}^{+(-)}(1) = ire^{+(-)i\Phi_s/2}, \tag{A1}$$

and the Andreev reflection amplitude of an incoming hole is given by $r_{eh}(1) = -r_{he}^*(1)$. Throughout this appendix we

consider trajectories that hit the NS interfaces any number of times, with the last hit occurring at the top interface. This is done for simplifying the calculation, and since the final result is even in Φ_s, it does not depend on this assumption. However, the treatment for trajectories that hit the interfaces an odd or an even number of times has to be done separately. For an odd trajectory, the recursion relation is

$$r_{he}(2N-1)=r_{he}^+(1)+\frac{r_{ee}^+(1)r_{he}(2N-2)r_{hh}^+(1)}{1-r_{eh}^+(1)r_{he}(2N-2)},$$
$$\text{(A2)}$$

where $r_{ee(hh)}^+(1)$ is the normal reflection of an electron (hole) from the upper NS interface. For an even trajectory the recursion relation is

$$r_{he}(2N)=r_{he}^-(1)+\frac{r_{ee}^-(1)r_{he}(2N-1)r_{hh}^-(1)}{1-r_{eh}^-(1)r_{he}(2N-1)}.$$
$$\text{(A3)}$$

We define

$$r_{he}(2N-1)=r_{he}^-(1)\frac{\beta_{2N-1}}{\gamma_{2N-1}}$$
$$\text{(A4)}$$

and

$$r_{he}(2N)=r_{he}^+(1)\frac{\beta_{2N}}{\gamma_{2N}}.$$
$$\text{(A5)}$$

Using the relations written after Eq. (5), we obtain

$$r_{he}(2N-1)=r_{he}^+(1)\frac{\beta_{2N-2}+\gamma_{2N-2}}{r^2\beta_{2N-2}+\gamma_{2N-2}},$$
$$\text{(A6)}$$

which we insert into Eq. (A3), and obtain the equation

$$\begin{pmatrix}\beta_{2N}\\\gamma_{2N}\end{pmatrix}=\begin{pmatrix}1+r^2e^{-i\Phi_s} & 1+e^{-i\Phi_s}\\r^2(1+e^{i\Phi_s}) & 1+r^2e^{i\Phi_s}\end{pmatrix}\begin{pmatrix}\beta_{2N-2}\\\gamma_{2N-2}\end{pmatrix}$$
$$=\begin{pmatrix}1+r^2e^{-i\Phi_s} & 1+e^{-i\Phi_s}\\r^2(1+e^{i\Phi_s}) & 1+r^2e^{i\Phi_s}\end{pmatrix}^N\begin{pmatrix}0\\1\end{pmatrix},$$
$$\text{(A7)}$$

where the last equation is obtained by explicitly finding that

$$\begin{pmatrix}\beta_2\\\gamma_2\end{pmatrix}=\begin{pmatrix}1+e^{-i\Phi_s}\\1+r^2e^{i\Phi_s}\end{pmatrix}.$$
$$\text{(A8)}$$

Following the same route for the odd case, we obtain

$$\begin{pmatrix}\beta_{2N+1}\\\gamma_{2N+1}\end{pmatrix}=\begin{pmatrix}1+r^2e^{i\Phi_s} & 1+e^{i\Phi_s}\\r^2(1+e^{-i\Phi_s}) & 1+r^2e^{-i\Phi_s}\end{pmatrix}\begin{pmatrix}\beta_{2N-1}\\\gamma_{2N-1}\end{pmatrix}$$
$$=\begin{pmatrix}1+r^2e^{i\Phi_s} & 1+e^{i\Phi_s}\\r^2(1+e^{-i\Phi_s}) & 1+r^2e^{-i\Phi_s}\end{pmatrix}^N\begin{pmatrix}e^{i\Phi_s}\\1\end{pmatrix}.$$
$$\text{(A9)}$$

Diagonalizing the matrices in Eqs. (A7) and (A9) we obtain for the odd case

$$R_{he}(2N+1,\Phi_s)=\left\{z+(1-z)\coth^2\left[y+N\,\tanh^{-1}\left(\frac{2r\cos(\Phi_s/2)\sqrt{(1-z)}}{1+r^2\cos\Phi_s}\right)\right]\right\}^{-1},\qquad\text{(A10)}$$

where

$$y=\tanh^{-1}\left(\frac{r\sqrt{(1-z)}}{e^{-i\Phi_s/2}+ir^2\sin(\Phi_s/2)}\right),\qquad\text{(A11)}$$

and for the even case Eq. (20). These equations are similar, only in the latter $y=0$.

APPENDIX B: VALIDITY OF THE CONDUCTANCE FORMULA FOR THE DIFFUSIVE SLAB

In Sec. VII we obtain the linear conductance of a diffusive NIS junction using the approximation that the electron's motion in the normal slab is deterministic. However, for a normal slab with short range disorder Beenakker et al.[32] obtain a formula which differs in the $\Gamma\gg T,T\to0$ limit by a factor of 2 from Eq. (23).

In order to understand the factor of 2 difference between the two cases we use the conductance formula for zero temperature of Beenakker et al.[22]

$$G_{NS}=\frac{4e^2}{h}\sum_{m=1}^n\frac{T_m^2}{(2-T_m)^2},\qquad\text{(B1)}$$

where T_m is the mth transmission eigenvalue of the normal slab.

The total transmission probability through the normal slab is given by $T=\sum_{m=1}^nT_m$. In our approximation of the long-range scattering potential, each electron entering the slab is predetermined, according to the position and direction at the entrance, to be either transmitted through the slab or reflected back to the normal reservoir (deterministic scattering). The transmission eigenvalues of the normal slab are therefore all zero and unity and in this case

$$\sum_{m=1}^n\frac{T_m^2}{(2-T_m)^2}=\sum_{m=1}^nT_m=T\qquad\text{(B2)}$$

and

$$G_{NS}=\frac{4e^2}{h}\sum_{m=1}^nT_m=\frac{4e^2}{h}T.\qquad\text{(B3)}$$

Since $G_N = (2e^2/h)\Sigma_{m=1}^n T_m$, we obtain the relation $G_{NS} = 2G_N$. However, in general, $T_m^2/(2-T_m)^2 < T_m$ for all $0 < T_m < 1$. In the case of short-range disorder the distribution of the transmission eigenvalues is such that $\Sigma_{m=1}^n T_m^2/(2-T_m)^2 = \frac{1}{2}\Sigma_{m=1}^n T_m = \frac{1}{2}T$,[22] and therefore $G_{NS} = (2e^2/h)T = G_N$. This results in a factor of 2 difference in the $T \to 0$ limit between our conductance formula (23) and the formula obtained by Beenakker *et al.*

APPENDIX C: LENGTH OF A DIFFUSIVE N TRAJECTORY: RANDOM WALK THEORY

We are interested in the question of how long a trajectory in the normal metal has to be in order to hit the interface N times. Looking at random walk in two dimensions on a lattice which is rotated by 45° from the coordinate axes, it is easy to see that, since we are not interested at the exact point the trajectory hits the interface, there is a one-to-one correspondence between returning to the interface in two dimensions and returning to the origin in the one-dimensional random walk. The question of return probabilities in one dimension is addressed in Ref. 35, Chap. 3, using random walk path theory. This approach is elementary and very instructive, and here we will just state its main results concerning our problem. Using path theory, Feller shows that in a one-dimensional random walk model, the probability of a first return to the origin after k steps is approximately, for large k, $f_k = (2\sqrt{\pi}k^{3/2})^{-1}$. Therefore, there is no average length for the first return ($\Sigma_{k=0}^\infty k f_k$ diverges). This peculiar result leads to a nonlinear dependence of the length of the trajectory on the number of times it hits the interface. (If there were an average return length α, then the average length of a trajectory that hits the interface N times would be αN.) It is further shown that the probability to hit the interface N times in a trajectory of length smaller than $\hat{L}$ is a function of $\hat{L}/N^2 l \equiv w$, where l is the mean free path and is given by

$$P(w) = \sqrt{\frac{2}{\pi}} \int_{w^{-1/2}}^\infty e^{-s^2/2} ds. \tag{C1}$$

This means that in order to hit the interface N times a particle has to travel a length of order $N^2 l$. A typical trajectory of length $N^2 l$ that hits the interface N times is not made of $N-1$ loops of similar length. The main contribution to the length of such a trajectory comes from one or two of its longest loops, whose lengths are of order $N^2 l$. This arises from the fact that $\Sigma_{k=N^2}^\infty f_k \approx 1/N$, which means that if we have N returns to the origin, about one of them is going to be longer than $N^2 l$. As N increases, we have probability of order 1 to have a loop of length $N^2 l$, and therefore the length of the longest loop, as well as the length of the whole trajectory, is of order $N^2 l$.

[1] A. Kastalsky, A. W. Kleinsasser, L. H. Greene, R. Bhat, and F. P. Milliken, Phys. Rev. Lett. **67**, 3026 (1991).

[2] C. Nguyen, H. Kroemer, and E. L. Hu, Phys. Rev. Lett. **69**, 2847 (1992).

[3] B. J. van Wees, P. de Vries, P. Magnée, and T. M. Klapwijk, Phys. Rev. Lett. **69**, 510 (1992).

[4] J. Nitta, T. Akazaki, H. Takayanagi, and K. Arai, Phys. Rev. B **46**, 14 286 (1992).

[5] H. Takayanagi, T. Akazaki, and J. Nitta, Phys. Rev. B **51**, 1374 (1995).

[6] H. Takayanagi, T. Akazaki, and J. Nitta, Phys. Rev. Lett. **75**, 3533 (1995).

[7] A. Dimoulas, J. P. Heida, B. J. v. Wees, T. M. Klapwijk, W. v. d. Graaf, and G. Borghs, Phys. Rev. Lett. **74**, 602 (1995).

[8] A. F. Morpurgo, S. Holl, B. J. van Wees, T. M. Klapwijk, and G. Borghs, Phys. Rev. Lett. **78**, 2636 (1997).

[9] A. F. Morpurgo, B. J. van Wees, T. M. Klapwijk, and G. Borghs, Phys. Rev. Lett. **79**, 4010 (1997).

[10] J. P. Heida, B. J. van Wees, T. M. Klapwijk, and G. Borghs, Phys. Rev. B **60**, 13 135 (1999).

[11] P. A. M. Benistant, H. van Kempen, and P. Wyder, Phys. Rev. Lett. **51**, 817 (1983).

[12] P. A. M. Benistant, A. P. van Gelder, H. van Kempen, and P. Wyder, Phys. Rev. B **32**, 3351 (1985).

[13] J. H. Schon, C. Kloc, R. C. Haddon, and B. Batlogg, Science **288**, 656 (2000).

[14] J. H. Schon, C. Kloc, and B. Batlogg, Nature (London) **406**, 702 (2000).

[15] E. V. Sukhorukov and I. B. Levinson, Sov. Phys. JETP **70**, 782 (1990).

[16] A. Kadigrobov, A. Zagoskin, R. I. Shekhter, and M. Jonson, Phys. Rev. B **52**, R8662 (1995).

[17] N. R. Claughton, R. Raimondi, and C. J. Lambert, Phys. Rev. B **53**, 9310 (1996).

[18] N. K. Allsopp, J. S. Canizares, R. Raimondi, and C. J. Lambert, J. Phys. J. Phys.: Condens. Matter **8**, L377 (1996).

[19] H. A. Blom, A. Kadigrobov, A. M. Zagoskin, R. I. Shekhter, and M. Jonson, Phys. Rev. B **57**, 9995 (1998).

[20] N. M. Chtchelkatchev, JETP Lett. **73**, 94 (2001).

[21] A. F. Morpurgo and F. Beltram, Phys. Rev. B **50**, 1325 (1994).

[22] C. Beenakker, Phys. Rev. B **46**, 12 841 (1992).

[23] M. Schechter, Ph.D. thesis, The Weizmann Institute of Science, 2001.

[24] G. Wendin and V. S. Shumeiko, Superlattices Microstruct. **20**, 569 (1996).

[25] V. T. Petrashov, V. N. Antonov, P. Delsing, and R. Claeson, Phys. Rev. Lett. **70**, 347 (1993).

[26] V. T. Petrashov, V. N. Antonov, P. Delsing, and R. Claeson, Phys. Rev. Lett. **74**, 5268 (1995).

[27] M. P. Anantram and S. Datta, Phys. Rev. B **53**, 16 390 (1996).

[28] J. Torres, T. Martin, and G. B. Lesovik, Phys. Rev. B **63**, 134517 (2001).

[29] A. L. Fauchere, G. B. Lesovik, and G. Blatter, Phys. Rev. B **58**, 11 177 (1998).

[30] C. W. Beenakker and H. van Houten, Phys. Rev. B **43**, 12 066 (1991).

[31] We thank Nathan Argaman and Doron Cohen for clarifying this point to us.

[32] C. W. J. Beenakker, B. Rejaei, and J. A. Melsen, Phys. Rev. Lett. **72**, 2470 (1994).

[33] A. Volkov, Physica B **203**, 267 (1994).

[34] F. Zhou, B. Spivak, and A. Zyuzin, Phys. Rev. B **52**, 4467 (1995).

[35] W. Feller, *An Introduction to Probability Theory and Its Applications* (Wiley, New York, 1966).